

Qualitative Aspects of the Phase Diagrams of $J_1 - J_2$ Model in the Cubic Lattice

Octavio D. R. Salmon ^{1,*} Nuno Crokidakis ^{2,†} Minos A. Neto ^{1,‡} Igor

T. Padilha ^{1,§} J. Roberto Viana ^{1,¶} and J. Ricardo de Sousa ^{1,3,**}

¹ *Departamento de Física, Universidade Federal do Amazonas,*

3000, Japiim, 69077-000, Manaus-AM, Brazil

² *Departamento de Física, PUC-Rio,*

Rua Marquês de São Vicente 225 22451-900 Rio de Janeiro - RJ, Brazil

³ *National Institute of Science and Technology for Complex Systems,*

3000, Japiim, 69077-000, Manaus-AM, Brazil

Abstract

The qualitative aspects of the phase diagram of the Ising model on the cubic lattice, with ferromagnetic first neighbors (J_1) and antiferromagnetic second neighbor couplings (J_2) are analyzed in the plane temperature versus α , where $\alpha = J_2/J_1$ is a frustrated parameter. We used the original Wang-Landau and the standard Metropolis algorithm to compare past results of this model obtained by the effective-field theory for the cubic lattice. Although the nature of some critical points, chosen at relevant values of α , show that the phase diagram is, in general, qualitatively correct, our Monte Carlo results suggest that the reentrance form of the frontier that separates the ferromagnetic and the colinear order is an artifact of the effective-field theory, which might disappear by improving these approach.

PACS numbers:

*octaviors@gmail.com

†nuno.crokidakis@fis.puc-rio.br

‡minosneto@pq.cnpq.br

§igorfis@ufam.edu.br

¶vianafisica@bol.com.br

**jsousa@edu.ufam.br

I. INTRODUCTION

Some magnetic compounds like $Eu_xSr_{1-x}S$ [1, 2] and $Fe_xZn_{1-x}F_2$ [3] present more than one low-temperature magnetic orderings, depending on its parameters, like the strength of the interactions and the concentration of magnetic ions x . They are well-described by models which consider competitions of nearest-neighbor and next-nearest-neighbor interactions. The simplest model which may describe such compounds is represented by the following spin hamiltonian:

$$\mathcal{H} = -J_1 \sum_{nn} \sigma_i \sigma_j + J_2 \sum_{nnn} \sigma_l \sigma_m, \quad (1)$$

where $\sigma_i = \pm 1$, and $i = 1, \dots, N$, where N is the total number of spins. The first sum contains all pairs of ferromagnetic nearest-neighbor couplings ($J_1 > 0$), and the second one is for all the next-nearest-neighbor antiferromagnetic interactions ($J_2 > 0$). The model with $J_2 \leq 0$, is well understood and establishes the Ising second-order universality class [4]. Nevertheless, this model has attracted a lot of interest in the past, especially when implemented in the square lattice [5–29]. For this case, the magnetic order at zero temperature depends on the value of the frustrated parameter $\alpha = J_2/|J_1|$. For $\alpha < 1/2$, the order is ferromagnetic (F, $J_1 > 0$) or antiferromagnetic (AF, $J_1 < 0$), and for $\alpha > 1/2$, we have the collinear order, also called superantiferromagnetic order (SAF). So, for $1/2 < \alpha \leq 1$, there has been controversial results about the nature of the order-disorder transition at finite temperatures. Recently, Kalz and Honecker [30] have concluded that Monte Carlo (MC) data, obtained with large sizes ($L = 1000, 2000$), yield a clear picture only for $1/2 < \alpha < 1$, where a first-order phase transition scenario is established by the double peaked structure of the energy histograms, and for $\alpha \geq 1$ there must be continuous phase transitions.

In the present work we study the model in Eq. (1), implemented on the cubic lattice with periodic boundary conditions, and $J_1 > 0$, $J_2 > 0$. This model has already been treated within an effective-field theory by dos Anjos et al. [31]. So, in Fig. (1), we show the phase diagram of this model in the plane $k_B T/J_1 - \alpha$, recalculated by the present authors using effective-field theory with a cluster of one central spin (EFT-1) as done in reference [31]. At zero temperature, it can be exactly determined two type of orderings separated by $\alpha = 1/4$. For $\alpha < 1/4$, the ferromagnetic order appears, whereas for $\alpha > 1/4$ a SAF order is set. At finite temperatures those phases are separated by a first-order frontier, which presents a

reentrant form, as shown in the inset of Fig. (1). This frontier finishes at a critical end point (CE), where two order-disorder frontiers are also ending. The first one is of second-order type and separates the F-Paramagnetic (P) transition, for lower values of α , and the second one is of first-order type and it separates the SAF-P transition, for higher values of α .

In that work, the authors used a decoupling procedure, which ignores all high-order correlations so as to approach the unmanageable expressions of all boundary spin-spin correlation functions. Although this analytical treatment improves the mean-field approach, which is insensitive to frustration, accuracy and qualitative aspects can be lost in determining the critical temperatures and the nature of the phase transitions. In order to verify the qualitative aspects of these phase diagrams, we need to use powerful Monte Carlo techniques to construct the canonical probability distribution function (CPDF) ($P(E, T) \sim \exp(-\beta E)$), for given temperatures, and finite sizes of the cubic lattice. Accordingly, at a critical temperature the *CPDF* will show a double-peaked form for a first-order phase transition, and a single-peaked form, for a second-order one. So, the original Wang-Landau sampling algorithm (WLS) is a suitable MC method to get the CPDF from density of states $g(E)$ [32, 33].

One of the advantage of this method is that we directly construct the density of states $g(E, T)$, through which the canonical partition function is achieved, so all the thermodynamic variables can be plotted as a temperature's function (free energy, heat capacity, etc). Furthermore, at low temperatures, the Metropolis algorithm will get trapped in states of energy local minima at low temperatures [34], especially in frustrated models. For instance, conventional simulations in the canonical ensemble would not be efficient in the region close to $\alpha = 1/4$ (see Fig. (1)), where the system is in a highly frustrated zone. Nevertheless, the original WLS is not without accuracy problems[35], however, it does not affect qualitative results. Another problem appears when larger lattice sizes are needed. In this case, we require to divide the relevant energy range into fixed windows, then we have to join them after convergence is achieved. Consequently, the resulting density of states and associated thermodynamic functions are shown to suffer from boundary effects. This undesirable effect becomes more conspicuous for the obtention of $g(E, M)$, which is useful to calculate the canonical probability distribution function including the order parameter $P(E, M, T)$. In this case, it is necessary to perform a two-dimensional random walk in a relevant (E, M) space. In most cases, this relevant (E, M) space needs to be divided by surfaces, but after

matching them the resulting $P(E, M, T)$ will have small discontinuities.

The general source of these difficulties seems to be due to the difficulty in matching surfaces at the boundaries rather than curves as in one-dimensional random walks [36]. To overcome this problem Cunha-Netto et al. proposed the WLS with adaptative windows [37], where instead of defining fixed energy windows, the boundary positions depend on the set of energy values on which the histogram is flat at a given stage of the simulation. So, errors that may arise near the border of a given window are corrected in subsequent stages, in which the border positions are shifted. Nevertheless, it improves the quality of the results of the *WLS* with fixed windows at the expense of computational cost. The *WLS* algorithm with adaptative windows considerably increases the computational time with the size of the system, and seems not to be able to be parallelized. Therefore, in this paper we use the multi-range original *WLS* algorithm with fixed windows, which does not affect qualitative results as will be shown.

II. METHODOLOGY

We used the original Wang-Landau algorithm so as to get the corresponding logarithm of the density of states ($\log g(E)$) for the model defined in Eq. (1). Consequently, we can calculate the mean energy E and specific heat curves C , and the canonical probability distribution functions $P(E)$ therefrom. These are our least necessary tools to do a qualitative analysis of the criticality of the system. In order to get $\log g(E)$, the minimum E_{min} and maximum E_{max} energies of the system are needed, for a given value of α and L . Then we also need to number every discrete energy value E_j between them to define an integer array $H(E_j)$ and a real array $g(E_j)$ as useful histograms for the algorithm. Initially, the $g(E)$ is unknown, so all bins in the array are set to unity. Since the typically range of $g(E)$ is of high orders of magnitude, it is common to store $\log g(E)$. In addition, a visits histogram $H(E)$ is maintained.

Initially, all bins have zero visits for both $\log g(E)$ and $H(E)$. The bins are then filled over the course of a MC simulation, in which moves (spin flips) are accepted if $p < \min \left\{ 1, \frac{g(E)}{g(E')} \right\}$, where p is a uniform random number in the range $[0, 1]$, E and E' are the energies of the current and the proposed move, respectively. After the move is accepted or rejected, the histogram $H(E)$ is incremented by one and the density of states histogram $g(E)$ is multiplied

by a constant factor f , such that $g(E) \rightarrow g(E) \times f$, where the initial choice is $f = e \simeq 2.72$. An accurate estimate of $g(E)$ is reached if the histogram $H(E)$ becomes flat.

At this step the histogram $H(E)$ is set to zero and the modification factor f is reduced such that $f_{i+1} \rightarrow \sqrt[n]{f_i}$. This process is repeated until f_i be close to 1, so we repeat it until $i = 14$, using $n = 4$ to accelerate the process. However, the repetition of the above simulation suffers from the shortcoming that very large entries need to be stored in $g(E)$. As mentioned before, in order to avoid this problem, the quantity $\log g(E) \rightarrow \log g(E) + \ln f$, is evaluated. The modification factor is then now updated as $\log(f_{i+1}) \rightarrow (1/n) \ln(f_i)$.

The adopted flatness criterion was $H(E_j) > 0.8 \langle H(E) \rangle$, $\forall j$. However, for the present model, it is difficult to satisfy it around $\alpha = 0.25$, on account of frustration. So, for a given f_i , we stop the process after a maximum number of Monte Carlo moves (M_{\max}). On the other hand, it is important to mention that it is not necessary to use the entire energy interval $[E_{\min} \dots E_{\max}]$ of the system to get the relevant information of the criticality. Thus, we need just to obtain the density of states for the relevant energy subspace $[E_1, E_2]$ in order to calculate the thermodynamic quantities throughout the temperature range of our interest. For our model, and for a given lattice size L , the number of energy bins are considerably increased for some values of α , this is why we have to apply a multi-range Wang-Landau algorithm with fixed windows even for the relevant energy subspace $[E_1, E_2]$. Otherwise, the flatness criterion will never be satisfied.

III. RESULTS AND DISCUSSION

We study the model defined in Eq. (1) by performing WLS and Metropolis algorithm for $0 \leq \alpha \leq 1$, for the cubic lattice with $N = L \times L \times L$ sites. We choose $L = 16$, because for $L > 16$ the number of energy bins are considerably increased for certain values of α . So, too many windows would be necessary to apply the multi-range WLS algorithm, which would also increase the computational cost. In Fig. (2a), it is shown the logarithm of the density of states $\log g(E)$, for $\alpha = 1.0$, for the entire energy space. This is an assymetric function in E , in contrast to that of the simplest spin-1/2 Ising Model.

Figure (2b) shows the corresponding mean energy and the specific heat versus temperature obtained therefrom. In Fig. (3), we show the CPDF for three different temperatures for $\alpha = 1$. A double-peaked structure appears at the estimated pseudo-critical temperature

showing a first-order phase transition. In Fig. (4) it is shown the energy range used to perform the WLS process for $\alpha = 0.5$ and for a given step of the algorithm ($i = 3$). There we may see the results for the four overlapped windows in which the selected energy range was divided. Then we meet the curves of the four windows into one curve to get the logarithm of the density of states plus a constant. Accordingly, in Fig. (5) we show the relevant results for $\alpha = 0.5$. In figure (5a) we see the specific heat curve in which both, WLS and traditional Metropolis simulations are in agreement. Accordingly, it is shown a first-order transition as presented in figure (5b). For $\alpha = 0.25$, the F and SAF orders coexist at $T = 0$. So, WLS results at finite temperatures present a first-order phase transition at the specific heat peak as shown in figures (6a) and (6b). It is necessary to point out that for this value of α , frustration gets the extreme, so traditional Metropolis simulations are not suitable to equilibrate the system, specially at low temperatures. This is why by the knowledge of the function of the density of states, obtained by WLS, one may overcome the limitations of the traditional Monte Carlo technique.

On the other hand, in order to verify whether a reentrant behavior occurs for the F-SAF frontier, as shown in Figure 1, we explored a closer value of α around 0.25, such as $\alpha = 0.24$. For this case, a relevant energy subspace requires many energy bins even for single temperature calculations. Accordingly, we had to construct the specific heat curve by sections within the WLS method. In figure (7a) we present these sections, which fit well with Traditional Metropolis simulations. At the specific heat peak, the corresponding CPDF shows a second-order phase transition in figure (7b), because a single-peaked structure appears. Furthermore, we explored the CPDF along the entire relevant range of temperatures and no double peak CPDF appeared for $\alpha = 0.24$, for this considered lattice size $L = 16$. So, this result strongly suggests that there is no reentrance for the F-SAF frontier. If that reentrance exist, it must be inside the interval $0.24 < \alpha < 0.25$. Consequently, we might infer that the reentrance shown in Fig. (1) be an artifact of EFT-1 approach. On the other hand, we may approximately locate empirically the end of the F-SAF frontier by observing the behavior of the orders parameters as functions of α , as shown in Fig. (8). So, by the aid of this figure we estimate the location of the CE point around $k_B T/J_1 = 1.0$, at $\alpha = 0.25$.

Finally, Fig. (9) shows the phase diagram of the present model in the plane $k_B T/J_1 - \alpha$, for $L = 16$. For $0 \leq \alpha < 0.25$ there is a second-order F-P critical frontier. On the other hand, for $0.25 \leq \alpha \leq 1$ there is a first-order SAF-P critical frontier. We affirm that the F-SAF frontier seems to be vertical. The three critical curves meet at a critical end point which must be around the end of arrow shown in this figure. Therefore, Fig. (9) shows a phase diagram which qualitatively agrees with that of the Fig. (1) obtained by EFT-1, with the exception of the reentrance appeared in it.

IV. CONCLUSIONS

The phase diagram of the Ising model in the presence of nearest- and next-nearest-neighbor interactions on a simple cubic lattice with $N = L \times L \times L$ sites, was studied by performing MC simulations considering the original WLS and the traditional Metropolis algorithm, for $L = 16$. The transition from the ferromagnetic phase to the disordered paramagnetic phase is of second-order type. On the other hand, a first-order transition frontier is suggested from the SAF phase to the P one, as well as from the SAF phase to the F one. The reentrance appeared in the F-SAF critical frontier obtained by an EFT-1 seems not to exist for the present model, at least out of $0.24 < \alpha < 0.25$. It suggests that this reentrance is a consequence of the nature of that approach. However, MC results give qualitatively the same phase diagrams as obtained by effective-field calculations.

ACKNOWLEDGEMENT This work was partially supported by CNPq (Edital Universal), CAPES, FAPERJ and FAPEAM (Programa Primeiros Projetos - PPP) (Brazilian Research Agencies).

-
- [1] H. Maletta, in *Excitations in Disordered Systems*, edited by M. F. Thorpe (Plenum Press, New York, 1982).
 - [2] H. Maletta, in *Heidelberg Colloquium on Spin Glasses*, edited by J. L. van Hemmen and I. Morgenstern, *Lecture Notes in Physics* Vol. 192 (Springer-Verlag, Berlin, 1983).

- [3] D. P. Belanger, in *Spin Glasses and Random Fields*, edited by A. P. Young (World Scientific, Singapore, 1998).
- [4] R.J. Baxter, *Exactly Solved Models in Statistical Mechanics* (Academic, London, 1982).
- [5] S. Katsura and S. Fujimori, J. Phys. C 7 (1974) 2506-2520.
- [6] M. N. Barber, J. Phys. A: Math. Gen. 12 (1979) 679-688.
- [7] F. Y. Wu, Phys. Rev. B 4 (1971) 2312-2314.
- [8] J. Oitmaa, J. Phys. A: Math. Gen. 14(1981) 1159-1168.
- [9] R. H. Swendsen and S. Krinsky, Phys. Rev. Lett. 43 (1979) 177-180.
- [10] D. P. Landau, Phys. Rev. B 21 (1980) 1285-1297.
- [11] K. Binder and D. P. Landau, Phys. Rev. B 21 (1980) 1941-1962.
- [12] D. P. Landau and K. Binder, Phys. Rev. B 31 (1985) 5946-5953.
- [13] J. L. Morán-López, F. Aguilera-Granja, and J. M. Sanchez, Phys. Rev. B 48 (1993) 3519-3522.
- [14] J. L. Morán-López, F. Aguilera-Granja, and J. M. Sanchez, J. Phys. Cond. Matter 6 (1994) 9759-9772.
- [15] C. Buzano and M. Pretti, Phys. Rev. B 56 (1997) 636-644.
- [16] K. Tanaka, T. Horiguchi, and T. Morita, Phys. Lett. A 165 (1992) 266-270.
- [17] J. A. Plascak, Physica A 183 (1992) 563-573.
- [18] P. M. Oliveira, C. Tsallis, and G. Schwachheim, Phys. Rev. B 29 (1984) 2755-2760.
- [19] H. W. J. Blöte, A. Compagner, and A. Hoogland, Physica A 141 (1987) 375-402.
- [20] M. P. Nightingale, Phys. Lett. A 59 (1977) 486-488.
- [21] H. W. Blöte and M. P. Nightingale, Physica A 134 (1985) 274-282.
- [22] P. A. Slotte, J. Phys. C 16 (1983) 2935-2951.
- [23] H. J. W. Zandvliet, Europhys. Lett. 73 (2006) 747-751.
- [24] F. Aguilera-Granja and J. L. Morán-López, J. Phys. Cond. Matter 5 (1993) A195-A196.
- [25] A. Malakis, P. Kalozoumis, and N. Tyraskis, Eur. Phys. J. B 50 (2006) 63-67.
- [26] J. L. Monroe and S.-Y. Kim, Phys. Rev. E 76 (2007) 021123-1021123-5.
- [27] A. Kalz, A. Honecker, S. Fuchs, and T. Pruschke, Eur. Phys. J. B 65 (2008) 533-537.
- [28] Rosana A. dos Anjos, J. Roberto Viana, and J. Ricardo de Sousa, Phys. Lett. A 372 (2008) 1180-1184.
- [29] A. OHare, F. V. Kusmartsev, and K. I. Kugel, Phys. Rev. B 79, 014439-8(2009).
- [30] A. Kalz and A. Honecker, Phys. Rev. B **84**, 174407(2011).

- [31] Rosana A. dos Anjos, J. Roberto Viana, J. Ricardo de Sousa and J. A. Plascak, Phys. Rev. E **76**, 022103(2007).
- [32] F. Wang and D.P. Landau, Phys. Rev. Lett. **86**, 2050(2001).
- [33] F. Wang and D. P. Landau, Phys. Rev. E **64**, 056101(2001).
- [34] Y. Okamoto, AIP Conf. Proc. 690, 248(2003).
- [35] A.A. Caparica, A.G. Cunha Netto, Phys. Rev. E **85**, 046702(2012).
- [36] Shan-Ho Tsai, F. Wang and D.P. Landau, Braz. J. Phys. **38**, 6(2008).
- [37] A. G. Cunha-Netto, A. A. Caparica, Shan-Ho Tsai, R. Dickman, and D.P. Landau, Phys. Rev. E **78**, 055701(2008).

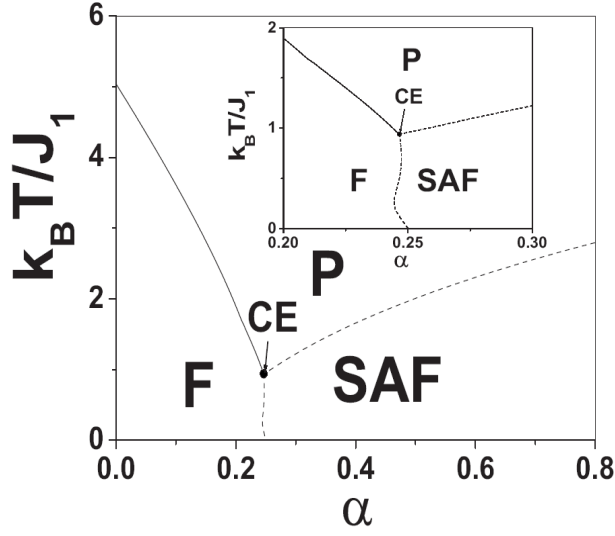


FIG. 1: Phase Diagram of the model described by the hamiltonian in Eq. (1). The vertical axis represents the reduced temperature, and the horizontal one represents the parameter of frustration ($\alpha = J_2/J_1$). Dashed and continuous lines represent first and second order critical frontiers, respectively. The inset shows better the reentrant form of the frontier separating the **F** and **SAF** orders. **CE** is the critical end point shown.

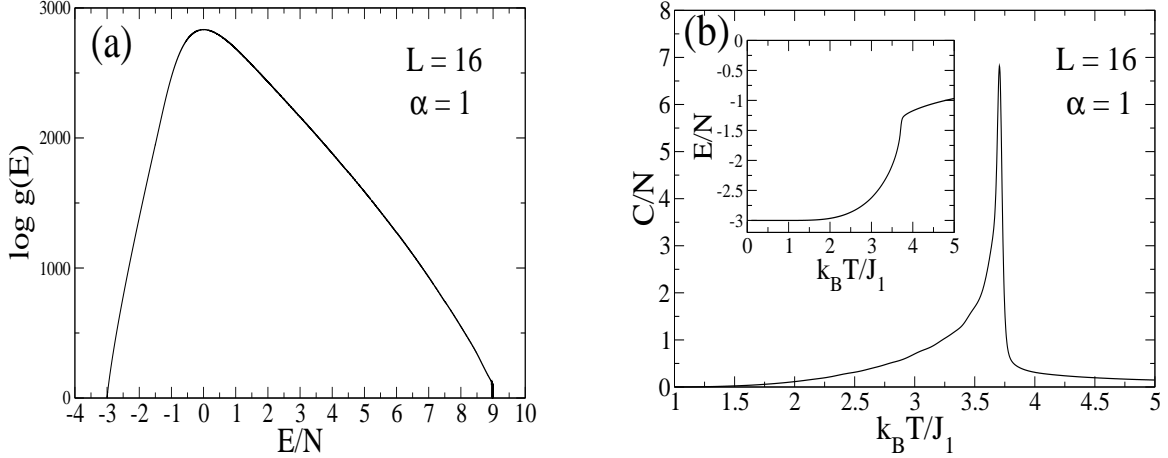


FIG. 2: (a) Logarithm of the density of states for $\alpha = 1$ and size $L = 16$, obtained by the original WLS algorithm applied for the whole energy range, without dividing it by windows. (b) Specific heat associated with the energy shown in the inset, which was obtained from the density in (a).

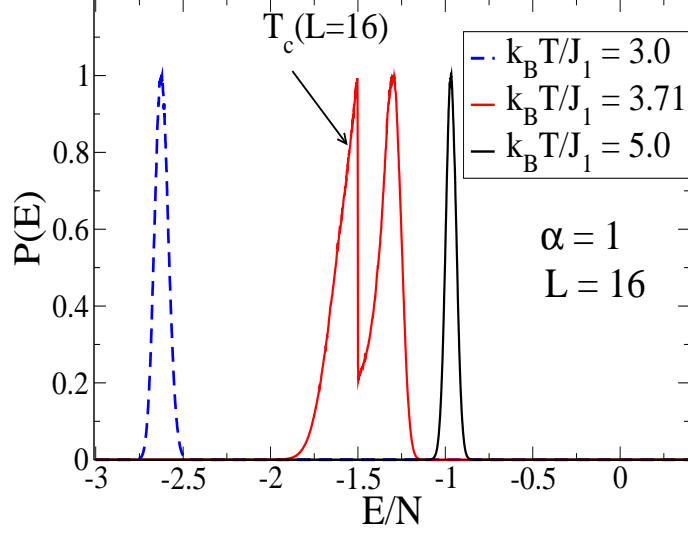


FIG. 3: CPDF for $\alpha = 1$ and size $L = 16$, at three different temperatures. This figure clearly shows a first-order phase transition because of the double peaked form of the CPDF at the pseudo-critical temperature for this lattice size.

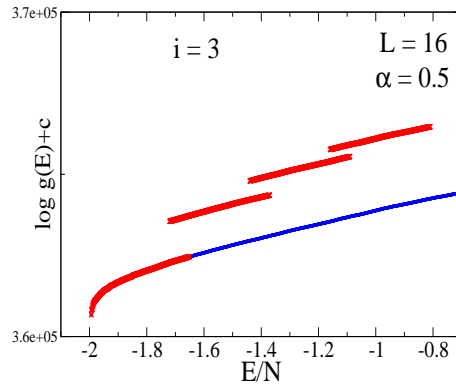


FIG. 4: Multi-range Wang-Landau results for the relative logarithm of the density of states, for $f_i = (\sqrt[4]{e})^i$, where $i = 3$. The blue curve represents the overlapped windows.

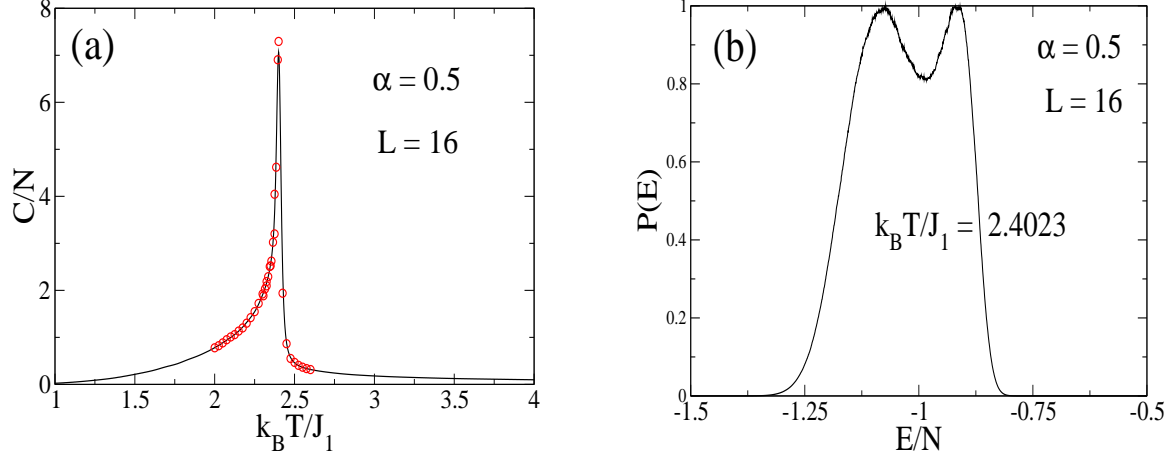


FIG. 5: (a) Specific heat for $\alpha = 0.5$ and $L = 16$. The continuous line corresponds to WLS simulations, whereas red points to traditional Metropolis ones. (b) CPDF at the pseudo-critical temperature.

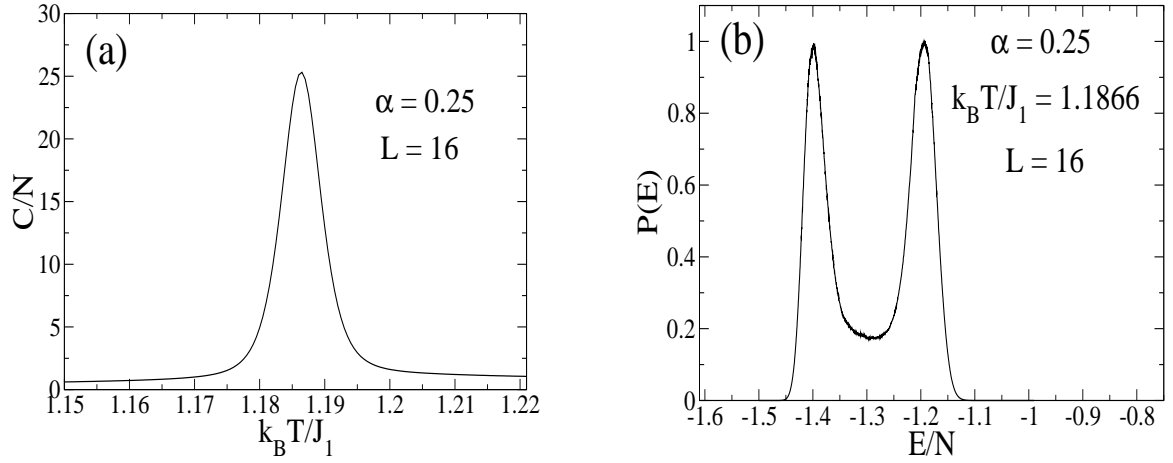


FIG. 6: (a) Specific heat for $\alpha = 0.25$ and $L = 16$. (b) CPDF at the corresponding pseudo-critical temperature.

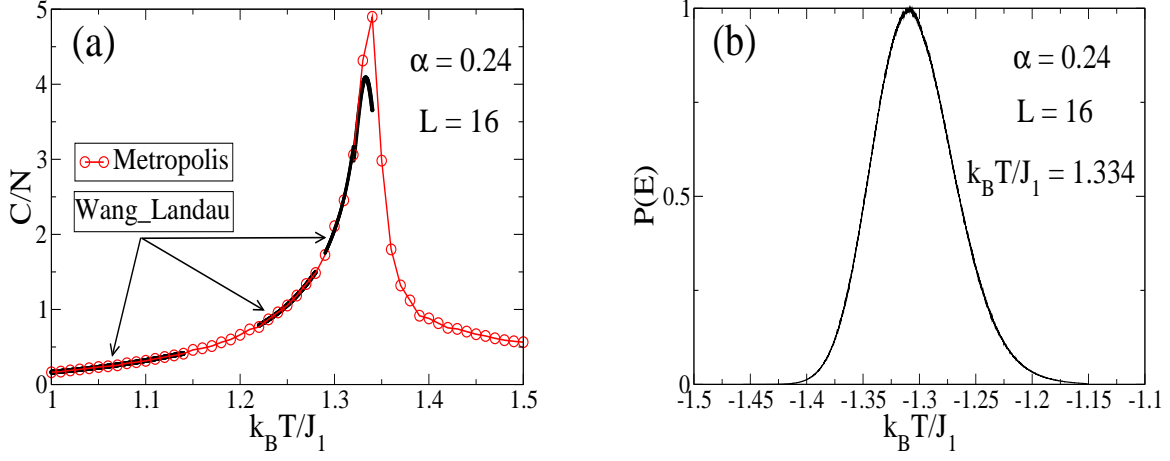


FIG. 7: (a) Specific heat for $\alpha = 0.24$ and $L = 16$. The black lines correspond to WLS results for different energy ranges, whereas red points to traditional Metropolis results. (b) CPDF at the corresponding pseudo-critical temperature for the specific heat peak obtained by WLS. The single peaked structure of the CPDF shows a second-order phase transition for the present size.

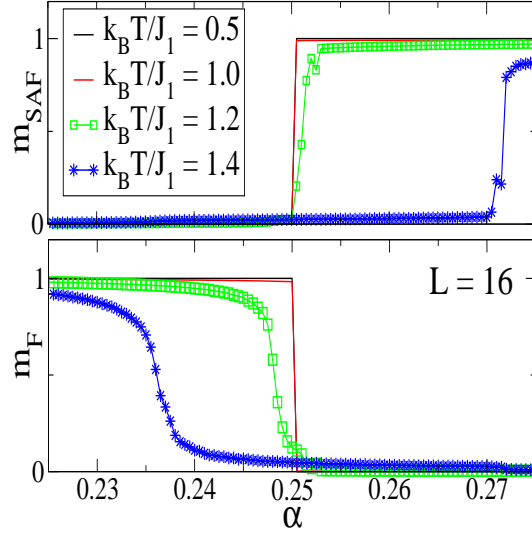


FIG. 8: Traditional Metropolis results for the order parameters versus α , for different temperatures.

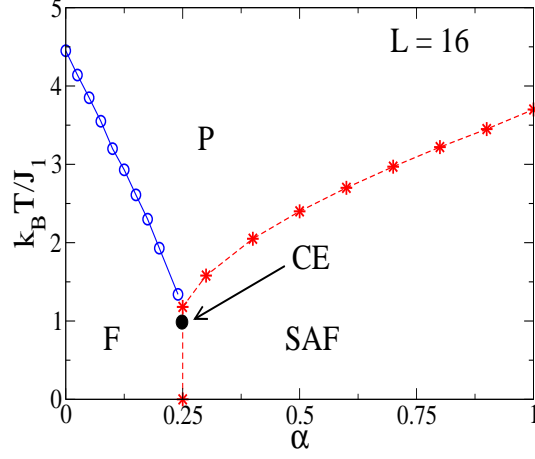


FIG. 9: Phase diagram of the model defined in Eq.(1) for $L = 16$. Circles represent estimated second-order critical points. Stars represent first-order critical points. The location of the critical end point is uncertain, so it must be close to the end of the arrow. The star at $T = 0$ and $\alpha = 0.25$ is exactly located. All lines are just guides to the visualization.